UC San Diego
UC San Diego Previously Published Works

Title

A parietal–frontal network studied by somatosensory oddball MEG responses, and its cross-modal consistency

Permalink

https://escholarship.org/uc/item/9510550s

Journal

NeuroImage, 28(1)

ISSN

1053-8119

Authors

Huang, Ming-Xiong
Lee, Roland R
Miller, Gregory A
et al.

Publication Date

2005-10-01

DOI

10.1016/j.neuroimage.2005.05.036

Peer reviewed

A parietal–frontal network studied by somatosensory oddball MEG responses, and its cross-modal consistency

Ming-Xiong Huang,[a,b,*] Roland R. Lee,[a,b] Gregory A. Miller,[c,d,e] Robert J. Thoma,[e,f] Faith M. Hanlon,[e,f] Kim M. Paulson,[f] Kimberly Martin,[f] Deborah L. Harrington,[a,g] Michael P. Weisend,[f] J. Christopher Edgar,[c] and Jose M. Canive[e,f]

[a]Department of Radiology, University of California, San Diego, San Diego, CA 92103-8756, USA
[b]Radiology Service, VA San Diego Healthcare System, San Diego, CA 92161, USA
[c]Department of Psychology and Beckman Institute Biomedical Imaging Center, University of Illinois at Urbana-Champaign, Urbana, IL 61801, USA
[d]Department of Psychiatry, University of Illinois at Urbana-Champaign, Urbana, IL 61801, USA
[e]Department of Psychiatry, University of New Mexico Health Sciences Center, Albuquerque, NM 87131-0001, USA
[f]Center for Functional Brain Imaging, New Mexico VA Health Care System, Albuquerque, NM 87131-0001, USA
[g]Research Service, VA San Diego Healthcare System, San Diego, CA 92161, USA

Previous studies using functional magnetic resonance imaging (fMRI) and event-related potentials (ERPs) of the brain have found that a distributed parietal–frontal neuronal network is activated in normals during both auditory and visual oddball tasks. The common cortical regions in this network are inferior parietal lobule (IPL)/supramarginal gyrus (SMG), anterior cingulate cortex (ACC), and dorsolateral prefrontal cortex (DLPFC). It is not clear whether the same network is activated by oddball tasks during somatosensory stimulation. The present study addressed this question by testing healthy adults as they performed a novel median-nerve oddball paradigm while undergoing magnetoencephalography (MEG). An automated multiple dipole analysis technique, the Multi-Start Spatio-Temporal (MSST) algorithm, localized multiple neuronal generators, and identified their time-courses. IPL/SMG, ACC, and DLPFC were reliably localized in the MEG median-nerve oddball responses, with IPL/SMG activation significantly preceding ACC and DLPFC activation. Thus, the same parietal–frontal neuronal network that shows activation during auditory and visual oddball tests is activated in a median-nerve oddball paradigm. Regions uniquely related to somatosensory oddball responses (e.g., primary and secondary somatosensory, dorsal premotor, primary motor, and supplementary motor areas) were also localized. Since the parietal–frontal network supports attentional allocation during performance of the task, this study may provide a novel method, as well as normative baseline data, for examining attention-related deficits in the somatosensory system of patients with neurological or psychiatric disorders.
© 2005 Elsevier Inc. All rights reserved.

Keywords: Oddball; MEG; Somatosensory; Median-nerve; Parietal–frontal network; P300; Dipole

Introduction

Attention mechanisms have been widely studied using the oddball paradigm, in which two visual or auditory stimuli are presented in a random order, and subjects discriminate rare target stimuli from standard, frequent stimuli. The P300 component of the human event-related potential (ERP) observed in auditory or visual oddball paradigms is one of the most widely studied ERP components. Using scalp or intracranial recordings, ERP studies have revealed a number of temporally overlapping, but anatomically distinct, cortical, and subcortical neuronal generators associated with the P300. These regions can be separated into three groups: (1) frontal regions, including anterior cingulate cortex (ACC), dorsolateral prefrontal cortex (DLPFC), and orbital frontal cortex (OFC) (Simson et al., 1976; Snyder et al., 1980; Yingling and Hosobuchi, 1984; McCarthy and Wood, 1987; Knight et al., 1989; Smith et al., 1990; Neshige and Luders, 1992; Baudena et al., 1995; Turetsky et al., 1989a,b; Anderer et al., 1998; Halgren et al., 1998; Wang et al., 2003); (2) temporal regions, including temporal lobes in general (Stapleton and Halgren, 1987; Halgren et

al., 1995a,b; Kiss et al., 1989; Wang et al., 2003) and specific temporal areas including the superior temporal gyrus (STG) (Knight et al., 1989; Lovrich et al., 1988; Tarkka et al., 1995; Halgren et al., 1998; Wang et al., 2003), medial temporal lobe (O'Donnel et al., 1993; Tarkka et al., 1995), hippocampus (Halgren et al., 1980, 1995b, 1998; Neshige and Luders, 1992), amygdala (Halgren et al., 1980; McCarthy and Wood, 1987), temporal–basal area (Hegerl and Frodl-Bauch, 1997), and temporal–parietal junction (Knight et al., 1989); and (3) parietal regions, including bilateral posterior parietal areas (Halgren et al., 1995a; Turetsky et al., 1989a,b; He et al., 2001), the lateral and inferior parietal cortex (Smith et al., 1990; Anderer et al., 1998; Halgren et al., 1998), and the parietal–occipital junction (Kiss et al., 1989; Anderer et al., 1998; Wang et al., 2003). These studies demonstrate that oddball paradigms evoke activity in distributed cortical and subcortical neuronal networks, although some deep structures (e.g., hippocampus and amygdala) might contribute less to the scalp P300 response (Johnson and Fedio, 1987; Smith et al., 1990; Halgren et al., 1995b). There also appears to be considerable sensory specificity with respect to brain activation during the task, for example, the involvement of the lateral temporal cortical regions in P300 responses may well be specific to auditory stimuli, since it has not been consistently observed in the visual oddball task. This was also shown by Rogers et al. (1992) using ERP and MEG, in which response to infrequent and unpredictable omissions of visual stimuli was localized deeply in the hippocampus/lateral thalamus, but not in temporal cortex.

Functional magnetic resonance imaging (fMRI) has also been used to localize regional activation during oddball tasks. With auditory, visual, or a combination of both oddball stimuli, fMRI methods verify that activity in distributed brain regions is elicited during the oddball task. One common goal of many studies is to distinguish cortical regions that do and do not depend on stimulus modality. Activation in the inferior parietal lobule (IPL)/supramarginal gyrus (SMG) and the ACC have been consistently reported in almost all fMRI studies using auditory and visual oddball tasks (McCarthy et al., 1997; Menon et al., 1997; Linden et al., 1999; Yoshiura et al., 1999; Stevens et al., 2000; Clark et al., 2000; Kiehl and Liddle, 2001; Ardekani et al., 2002). Activation in DLPFC and middle frontal gyrus (MFG) is also frequently reported in fMRI studies and appears modality-independent (McCarthy et al., 1997; Yoshiura et al., 1999; Clark et al., 2000; Stevens et al., 2000; Kiehl and Liddle, 2001; Ardekani et al., 2002).

Together, ERP and fMRI research indicate that a distributed parietal–frontal network is commonly activated during both auditory and visual oddball tasks. This network involves frontal regions such as DLPFC/MFG and ACC, and parietal cortex, including the IPL/SMG. In addition, this network appears to be modality-independent, consistent with its involvement in verbal and nonverbal working memory (McCarthy et al., 1997; Goldman-Rakic, 1987, 1988; Mesulam, 1990). On the other hand, the temporal cortex and occipito-temporal areas appear to be modality-dependent because activity is more commonly evoked only by auditory oddball tasks.

The present study investigated neuronal networks that support attention to somatosensory stimuli. In contrast to auditory and visual oddball tasks, the neuronal network involved in oddball responses evoked by somatosensory stimuli has not been well studied. Most research has focused on somatosensory recognition by using spatial attention tasks, which stimulate different body parts (Desmedt and Tomberg, 1989; Garcia-Larrea et al., 1995;

Hari et al., 1990; Tarkka et al., 1995; Kekoni et al., 1996; Mauguiere et al., 1997b; Yamaguchi and Knight, 1991), the same body part (i.e., median-nerve) but with different stimulation intensities, (Mima et al., 1998), or a mix of somatosensory and auditory stimuli (Fujiwara et al., 2002). Neuronal responses in primary and secondary somatosensory regions have been the focus of these investigations.

Although recently parietal–frontal networks have figured centrally in theories of brain mechanisms associated with selective attention (e.g., Milham et al., 2003), we are not aware of any research studying the role of parietal–frontal networks in somatosensory attention during oddball paradigms. Thus, it is not clear whether this network is truly modality-independent. This is important because if similar parietal–frontal networks support attention during somatosensory processing, this would have implications for using somatosensory tasks to evaluate cortical function in neurological patients with limited capacity for movement (Huang et al., 2004a,b). The present study used a novel oddball paradigm involving median-nerve stimulation to investigate the broader role of the cerebral cortex in attending to somatosensory stimuli. MEG was used to identify the locations of multiple cortical neuronal generators and their time-courses with millisecond (ms) temporal resolution. Although one fMRI study reported that activity in the IPL and SMG begins earlier than DLPFC/MFG activity (Stevens et al., 2000), the precise onset latency could not be determined due to the slow hemodynamic response of the fMRI signal. This is especially problematic when studying the somatosensory system, where considerable neuronal activity occurs within the first 100 ms.

Millisecond temporal resolution can be also obtained from intracranial and scalp EEG/ERP recordings. However, intracranial ERP is invasive and can only be performed at limited sites in surgical candidates. A limitation of scalp ERP is its relatively low spatial resolution and localization accuracy, relative to MEG, even when using a high-density electrode array (Leahy et al., 1998). This is mainly due to errors in EEG in estimating and modeling the conductivity profile of the head, especially the substructure of the skull (Leahy et al., 1998). In contrast, for relatively superficial and focal neuronal generators, spatial localization accuracy and resolution of MEG can be on the order of a few millimeters in the auditory (Romani, 1986; Pantev et al., 1995), somatosensory (Kawamura et al., 1996; Huang et al., 2000), and visual modalities (Aine et al., 2000; Stephen et al., 2002). In theory, the spatial resolution of neuronal activity in MEG appears to be limited to a few millimeters due to primarily the head movement and registration error between MEG and anatomic images.

We hypothesized that the same parietal–frontal network activated by auditory and visual oddball tasks (specifically IPL/SMG, ACC, and DLPFC) would also be more activated for rare than frequent somatosensory stimulation in our MEG median-nerve oddball task, if this network is indeed modality-independent. We also hypothesized that the time-course of activity in the IPL/SMG would precede activity in the ACC and DLPFC, if the parietal cortex modulates attention to somatosensory information, perhaps during early stages of working memory (McCarthy et al., 1997; Halgren et al., 1998). Furthermore, we predicted that somatosensory-dependent regions, including primary somatosensory (SI) area, bilateral secondary somatosensory areas (SII), dorsal premotor area (dPMA), primary motor area (M1), and supplementary motor area (SMA), would also be more activated by

selective attention to somatosensory information. Finally, processing in these somatosensory-dependent regions was predicted to precede processing in the ACC and DLPFC components of the parietal–frontal network given their role in higher-level cognitive functions that act upon sensory information.

Material and methods

Subjects

Nine right-handed subjects (7 males, 2 females) without neurological or psychiatric disorders were recruited from the Albuquerque area. Their mean age was 39.3 years (SD = 13.9 years). All subjects signed consent forms approved by the Human Research Review Committee of the University of New Mexico.

Median-nerve oddball task

Subjects performed a novel oddball task involving median-nerve stimulation as they underwent MEG. During the task, strong but painless electrical stimulation was applied to the right and left median nerves via electrode pairs taped to each wrist with electrode separation of 2 cm. The stimuli were square-wave electric pulses (0.25 ms duration) generated by a bipolar GRASS stimulator. The intensity of the stimulation was adjusted until robust thumb twitches were achieved. A trigger from the stimulator, simultaneous with the stimulus, was sent to the MEG acquisition system for signal averaging.

Stimuli were presented in series of 4 blocks, such that Blocks 1 and 3 were the same, as were Blocks 2 and 4. A diagram of the organization of Blocks 1 and 2 is shown in Fig. 1. In Blocks 1 and 3, 15% of the stimuli were delivered to right wrist and 85% to the left wrist. Subjects were instructed to count silently the rare stimuli to the right wrist. In Blocks 2 and 4, 85% of the stimuli went to the right wrist and 15% to the left wrist; subjects were instructed to count the rare stimuli on the left wrist. The inter-stimulus interval was 1000 ms. After each block, the number of rare stimuli counted by the subject was recorded and compared with the exact number of the rare stimuli recorded in the raw MEG file to assess the performance of the subject during the test. MEG trials from Blocks 1 and 3 were concatenated, as were the trials from Blocks 2 and 4, after discarding trials with artifacts (e.g., eye-blinks, large eye-movements, etc.). On each wrist, 150 trials of rare MEG responses, and about 850 trials of frequent responses, were collected for each subject and averaged to create two averaged files, one for rare and one for frequent responses. Then for each side, the rare and frequent MEG conditions were compared as indicated by arrows in Fig. 1. The order of Blocks 1 and 2 (and accordingly Blocks 3 and 4) was randomized across subjects.

In previous somatosensory oddball studies, the rare and frequent conditions were either different modalities (e.g., somatosensory and auditory, or somatosensory and visual), the same modality (i.e., somatosensory) with different stimulation sites on the body, or the same stimulation site with different stimulation intensities (Desmedt and Tomberg, 1989; Garcia-Larrea et al., 1995; Hari et al., 1990; Kekoni et al., 1996; Mauguiere et al., 1997b; Yamaguchi and Knight, 1991; Mima et al., 1998; Fujiwara et al., 2002). To better equate rare and frequent stimuli, we used a single somatosensory modality and stimulus intensity for rare and frequent stimuli (indicated by arrows in Fig. 1), which were delivered to the same body site. In other words, all stimuli-related parameters in our design were identical and the only difference was the subject's focus of attention. This design avoided confounding attention to different modality-types and other stimulus-specific parameters (e.g., site, intensity, etc.), and also detection of attention-related changes by directly subtracting frequent and rare responses obtained from the same stimulation site.

MEG and anatomical MRI data acquisition and co-registration

Brain responses were recorded by an Elekta-Neuromag whole-head MEG system (Helsinki, Finland) with 122 planar gradiometers in a magnetically-shielded room (IMEDCO-AG, Switzerland). Two pairs of EOG electrodes were used to detect eye blinks and eye movements. Trials coincident with eye blinks and large eye movements were not included in the averaged file. During the 4-block recording session, precautions were taken to ensure head stability: Foam wedges were inserted between the subject's head and the inside of the unit. A Velcro strap was also placed under the subject's chin, and anchored superiorly and posteriorly.

For each epoch, an interval of 500 ms post-stimulus was selected when creating the averaged response from the raw MEG data, and a 300-ms pre-stimulus interval was used for noise estimation and baseline correction. The A-to-D sampling frequency of the data was 1000 Hz, and the data were run through a high-pass filter with 0.1 Hz cut-off, a low-pass filter with 300 Hz cut-off, and through a notch filter (58–62 Hz) to remove 60 Hz power-line noise.

To aid in MEG source modeling, 3D volumetric magnetic resonance images (MRI) were acquired in a 1.5-T Picker/Phillips scanner. The pulse sequence was a Gradient Echo 3-D sagittal sequence (TR, 15 ms; TE, 4.4 ms; FOV, 256 mm; 192×256 matrix; flip angle, 25°; slice thickness, 1.5 mm, no gap). Whole-head coverage was provided by 128 slices.

To co-register the MEG with MRI, three small coils were attached to each subject's head during the preparation phase of each MEG session. A Polhemus system was used to digitize the location of the coils and three anatomical landmarks (i.e., nasion, left and right preauricular). The coils were activated briefly by

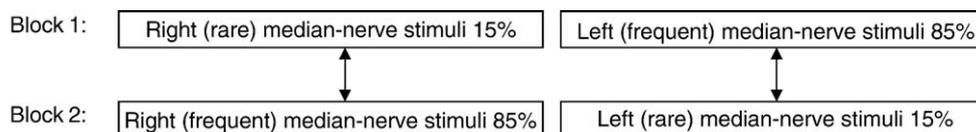| Block 1: | Right (rare) median-nerve stimuli 15% | Left (frequent) median-nerve stimuli 85% |
| Block 2: | Right (frequent) median-nerve stimuli 85% | Left (rare) median-nerve stimuli 15% |

Fig. 1. Median-nerve oddball paradigm. Block 1, 15% of the stimuli were delivered to right wrist and 85% to the left wrist. Subjects were instructed to count silently the rare stimuli to the right wrist. Block 2: the rare and frequent stimuli were reversed, and the subjects were instructed to silently count the rare stimuli on the left wrist. For each side, the oddball MEG signals were obtained by subtracting the frequent responses from the rare responses across different blocks as indicated by the arrows. Block 3 was identical to Block 1 and Block 4 was identical to Block 3.

sinusoidal current at the beginning and the end of each MEG data acquisition session to specify the position and orientation of the MEG sensors relative to the head. By identifying the same anatomical landmarks on the subject's MR images, using Neuromag (Helsinki, Finland) software, a transformation matrix involving both rotation and translation between the MEG and MRI coordinate systems was generated to provide proper co-registration of the MEG functional localizations to the anatomical structure. To increase the reliability of the MEG-MRI co-registration, approximately 80 points on the scalp were digitized with the Polhemus system, in addition to the three landmarks, to ensure that all points were located on the MRI scalp surface. Based on our previous experience, the MEG-MRI co-registration error in the present study was expected to be less than 3 mm (Leahy et al., 1998).

MEG signal processing

A spherical MEG head model was adopted (Sarvas, 1987). In this approach, a sphere was fitted to the inner surface of the skull using each subject's MRI. It was shown that for sensorimotor cortices, the spherical model and the real-shape head model based on the boundary element method (c.f. Mejis et al., 1987; Hämäläinen and Sarvas, 1989; Ferguson et al., 1994; Schlitt et al., 1995) yielded very similar results, due to the high spherical symmetry of the skull in this region (Leahy et al., 1998). The widely-adopted equivalent-current-dipole model, which assumes that brain activations are focal and can be modeled by a few point current dipoles, was applied in the present study. The physiological validity of the dipole model for early somatosensory responses has been well documented (Okada et al., 1996; Jenkins and Merzenich, 1987). For the late somatosensory oddball response, brain activation may not be as focal, and the multiple-dipole model may only approximate the centroid of larger distributed sources.

The dipole locations were determined by a non-linear multiple dipole fitting procedure, and the linear dipole moment parameters were obtained through a linear fit for given dipole locations. As with other available functional brain imaging methods, MEG source localization relies on evolving methods and considerable judgment. Our group takes several steps to provide reliable localization results, including the automated multi-dipole localization technique. This method is called multi-start spatio-temporal or MSST algorithm (Huang et al., 1998). In this algorithm, downhill simplex searches (Nelder and Meed, 1965) are performed many times, usually a few thousand for multiple dipoles, for a given model order (i.e., the number of dipoles to fit). Each time, the program selects a set of starting dipole locations by randomly sampling a user-selected search volume (Huang et al., 1998). This method has been tested in computer simulations, phantom studies, and human studies, and has been shown to be a significant improvement over traditional inverse techniques in terms of source localization accuracy and ability to model previously unknown and/or weak sources (Huang et al., 1998, 2000, 2004a,b; Aine et al., 2000; Shih et al., 2000; Stephen et al., 2002, 2003; Hanlon et al., 2003). Unlike the traditional multi-dipole fitting approaches, MSST does not require users to provide initial guesses for dipole locations so the fitting procedure is more objective.

Determining the adequate number of dipoles to model the data (model order) is an important procedure in any multiple-dipole fitting method. Great care has been taken in MSST to ensure the data are not under modeled (the number of dipole is less than

adequate) or over modeled (more than adequate number of dipoles used). First, singular value decomposition (SVD) (Golub and Van Loan, 1984) was used to obtain the number of asynchronous
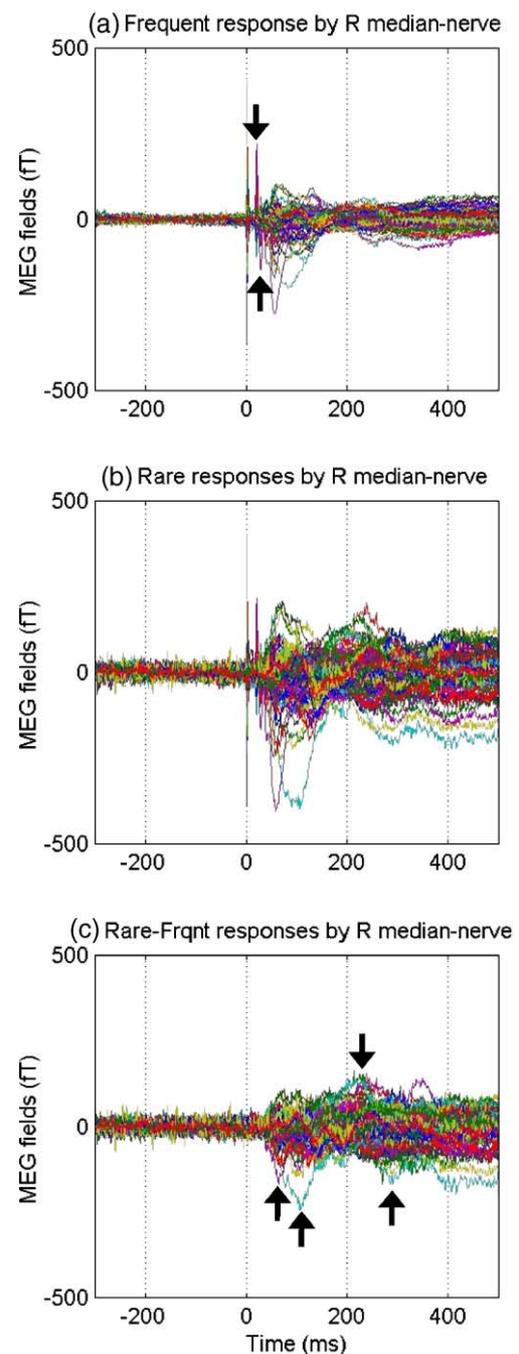

Fig. 2. MEG sensor waveforms from 122 channels in a representative subject evoked by the median-nerve oddball test averaged over about 850 "frequent" trials and 150 "rare" trials. (a) Sensor waveforms evoked by the frequent stimuli delivered to the subject's right median-nerve. The two arrows indicate the sharp N20 m and P30 m components. (b) Sensor waveforms evoked by the rare stimuli delivered to the right median-nerve. Note the marked increase in averaged signal amplitude. Because there were fewer rare trials than frequent trials, the signal-to-noise was worse than in (a). (c) Sensor waveforms of rare minus frequent oddball responses. Arrows indicate the components with large signal enhancement. Note that the N20 m and P30 m are not visible in this difference-waveform plot.

sources (the number of signal-related singular values, which reflects the minimum model order) for a given interval of data (De Munck, 1990; Berg and Scherg, 1994; Huang et al., 1998). If the noise in the data was white (uncorrelated), the SVD plot of singular values against index number is "L"-shaped, with the signal-related singular values in the part with the larger slope and the noise-related singular values in the part with the smaller slope. In this case, obtaining the signal-related singular values from SVD is straightforward. However, if there is some correlated noise in the data, the transition between noise-related singular values and the signal-related singular values is gradual. In this case, the data were pre-whitened (Knösche et al., 1998; Hansen, 1997, Sekihara et al., 1997, 1999) before the number of asynchronous sources was determined from the SVD. Next, to derive the adequate model order, a search beyond the minimum model order was performed to account for synchronous or near-synchronous sources that may exist (Huang et al., 1998, 2000, 2004b; Aine et al., 2000). For a given model order, the reduced χ^2 (χ^2 normalized by the number of degrees of freedom) was used as the goodness-of-fit measurement, in which the noise variance is estimated from the pre-stimulus interval. An adequate model order was found when all of the following criteria were satisfied: (1) an increase in the model order

did not significantly lower the reduced χ^2 values, but a decrease in the model order significantly increased the reduced χ^2 values; (2) the best-fitting MSST solutions with similar reduced χ^2 values (within 5% of each other) formed clusters in a dipole-location plot; and (3) no signal remained in the fitted residual (i.e., the difference between the empirical data and the modeled data).

A Monte-Carlo analysis (Medvick et al., 1989) was used to provide the statistical uncertainty of the dipole solutions from MSST. In this procedure, 300 sets of simulated Gaussian random noise were added to the modeled MEG fields created by the best-fitting MSST solution. The variance of each set of the random noise was set to be the same as the -300 ms to -5 ms pre-stimulus noise interval. The noisy data were fitted back with the same model order as the fit of the original data using a downhill simplex direct search algorithm, and the perturbations in dipole location due to noise were obtained.

Talairach coordinates

To compare our MEG source locations with those reported in auditory and visual oddball fMRI studies, we obtained the Talairach coordinates (Talairach and Tournoux, 1988) of the MEG sources
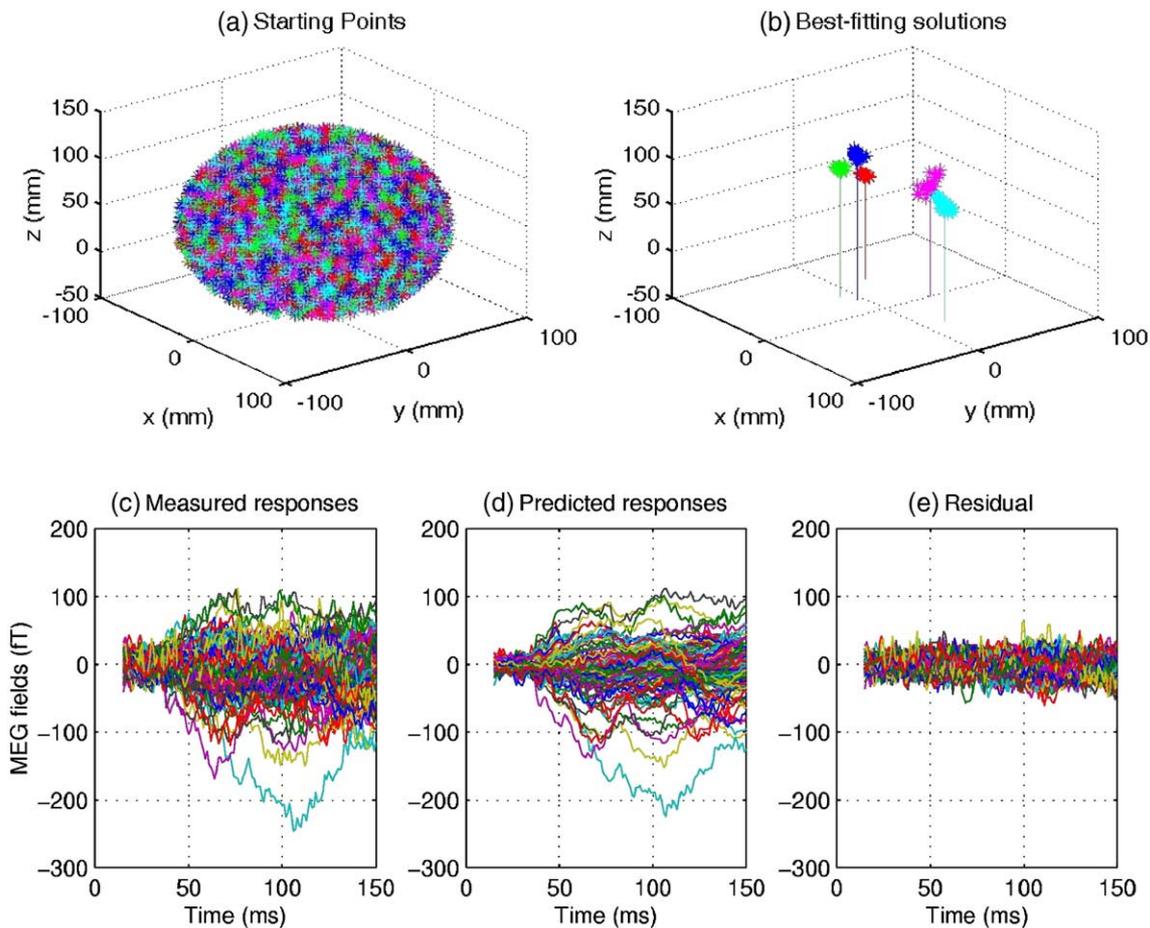

Fig. 3. An example demonstrating the general procedures for analyzing MEG data using MSST. Data are from the 15–150 ms interval for the subject reported in Fig. 2. (a) In localizing 5 dipoles, 3000 sets of starting locations were selected randomly by sampling a searching volume. Each set contains 5 dipole locations indicated by 5 different colors. (b) The 20 best-fitting MSST solutions formed 5 clusters for this 5-dipole fit. Vertical lines are drawn to delineate the centroids of the clusters. (c) Measured MEG sensor waveforms of right arm median-nerve oddball responses (rare minus frequent stimuli) for the 15–150 ms interval in the same subject. (d) The predicted (calculated) sensor waveforms based on the best-fitting 5-dipole solutions. (e) The residual, the difference between the measured and predicted sensor waveforms.

using the brain normalization software in the SPM2 (http://www.fil.ion.ucl.ac.uk/spm/software/spm2/), which uses a 12-parameter affine transformation and a nonlinear deformation (Friston et al., 1995; Ashburner et al., 1997; Ashburner and Friston, 1999). In this approach, the 3 fiducials (left PA, right PA, NA) of each individual subject's MRI were first identified using SPM2's MRI display function to create a transformation between the MEG source coordinate system and the MRI coordinate system. This step is the same as the co-registration procedure mentioned previously with the Neuromag software. Then, SPM2 was used to normalize the subject's MRI into Talairach space and obtain a second transformation. By combining these two transformations, Talairach coordinates of the MEG sources for each individual subject were obtained.

Results

Detailed source analysis using MSST

Performance of all subjects was highly accurate, with a correct counting rate of 97.6 ± 1.7% (mean ± SD). Fig. 2a shows the trial-averaged MEG sensor waveforms evoked by the frequent stimuli delivered to one representative subject's right median-nerve. The MEG waveforms from 122 channels are superimposed. The spike at 0 ms is the stimulus artifact. The first and second sharp peaks at 20 ms and 30 ms with different polarities are the N20 m and P30 m (the magnetic counterparts of the N20 and P30 in ERP) cortical components, which are generated mainly from primary somatosensory (Wood et al., 1985; Allison et al., 1991a,b; Hari et al., 1993; Forss et al., 1994; Kawamura et al., 1996; Mauguiere et al., 1997a,b; Forss and Jousmaki, 1998; Jousmaki and Forss, 1998; Hari and Forss, 1999; Huang et al., 2000, 2004a) and primary motor cortices (Rosen and Asanuma, 1972; Lemon and Porter, 1976; Jones et al., 1978, 1979; Wong et al., 1978; Lemon and van der Burg, 1979; Asanuma et al., 1980; Lemon, 1981; Davidoff, 1990; Baldissera and Leocani, 1995; Kawamura et al., 1996; Spiegel et al., 1999; Huang et al., 2000, 2004a; Balzamo et al., 2004). In Fig. 2b, the rare MEG responses from the same subject are plotted. The signals in the rare condition showed a marked increase in many components, compared with the frequent condition. Since a major focus of the present study was the locations and time-courses of the components that show differences between the rare and frequent conditions, the difference–waveform (rare minus frequent stimuli) is plotted in Fig. 2c. This graph shows that the sharp N20 m and P30 m disappeared in the difference–waveform plot, a strong indication that these components are unaltered by attention during our median-nerve stimulation oddball test. Unlike the earlier components, later components showed marked increases as highlighted by arrows in Fig. 2c.

Because we expected that a large number of generators would be involved in the MEG oddball response (rare minus frequent stimuli), we first divided the entire post-stimulus session into three smaller epochs for the rare-minus-frequent averaged file: (1) 15–150 ms interval, (2) 150–250 ms interval, and (3) 250–
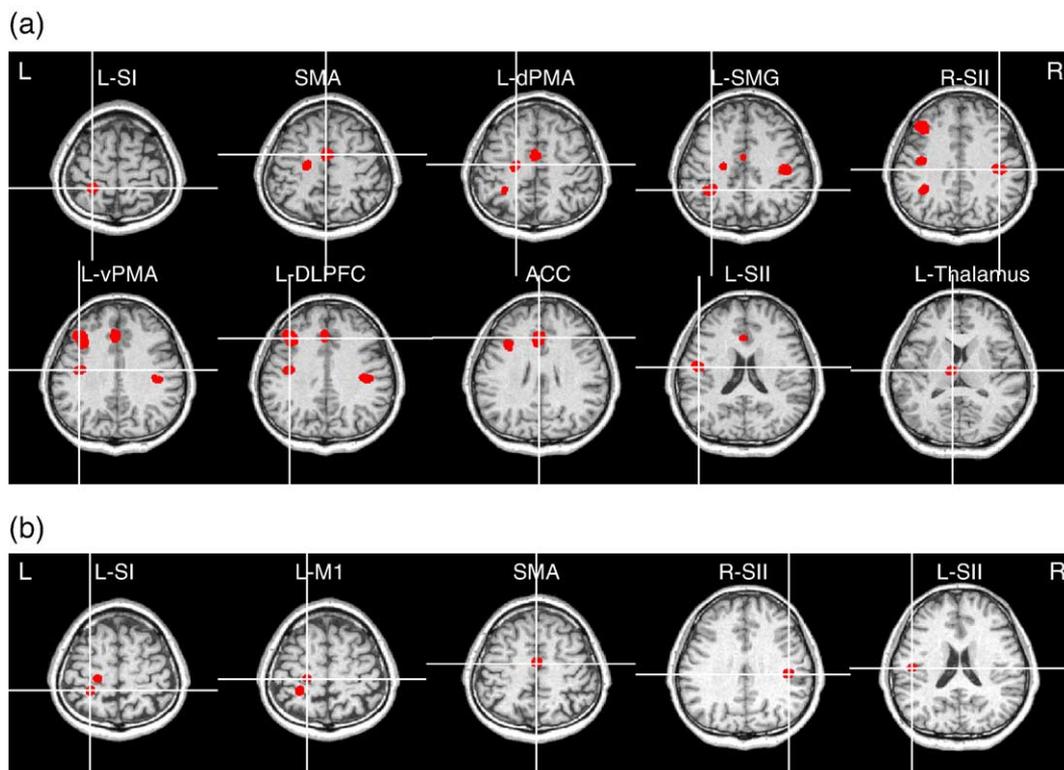

Fig. 4. (a) Ten neuronal generators showing activation during the 15–500 ms interval in the same representative subject's right arm median-nerve oddball responses (rare minus frequent stimuli). The clusters indicate the localization uncertainty determined by Monte-Carlo analysis. These sources from superior to inferior slices, under the cross-hairs are: left SI, midline SMA, left dPMA, left SMG, right SII, left vPMA, left DLPFC, midline ACC, left SII, and left thalamus. Neurological convention was adopted. (b) Five sources active in the 15–500 ms following frequent stimulation to the right arm: left SI, left M1, midline SMA, right SII, and left SII.

500 ms interval. MSST was used to localize the neuronal sources and obtain their time-courses for each interval. These intervals were selected to study the early somatosensory responses, the M300 (the analog of P300) responses, and a mid-interval which is often used to study mismatch negativity in ERPs, respectively. Then, all non-redundant generators from the three intervals were used in a final fit to the entire 15–500 ms interval to obtain the final source locations and their time-courses for the whole interval.

Fig. 3 demonstrates the general procedures for analyzing MEG data using MSST and the responses evoked by right median-nerve stimulation on the same representative subject. The algorithm performed a downhill simplex search (Nelder and Meed, 1965) 3000 times for a given model order of 5 (i.e., the number of dipoles to fit). Each time, the program selected a set of starting dipole locations (i.e., starting points) by randomly sampling a user-selected search volume (Huang et al., 1998). Fig. 3a shows that to fit the MEG responses with the 5 dipoles, the 3000 sets of starting locations were selected by randomly sampling a searching volume, which was specified by a spherical shell: the ranges for ρ (radius), θ (elevation angle), and ϕ (azimuth angle) are 20–90 mm, 0–

140°, and 0–360°, respectively. Each set contains 5 dipole locations indicated by 5 different colors in the plot. The MEG difference-responses (rare minus frequent) evoked by the right median-nerve oddball test were fit by a five-dipole model. Fig. 3c shows the measured magnetic fields for the 15–150 ms interval, in which the MEG difference waveforms from 122 channels are superimposed (i.e., a "zoomed-in" version of Fig. 2c). This figure indicates that many channels show activation between the first component at about 60 ms and the second component at around 100 ms in Fig. 3c.

After multiple searches were performed, the sets of best-fitting solutions with similar reduced χ^2 values (i.e., in this case the 20 best-fitting sets) formed 5 clusters for the 5-dipole fit, as shown in Fig. 3b. The centroid of each cluster was taken as a dipole location, indicated by the x, y, and z coordinates of the vertical lines in Fig. 3b. These 5 dipoles were localized to SI, SII, SMG, SMA, all in the left (contralateral) hemisphere, and ipsilateral SII in the right hemisphere (see next paragraph). The predicted (calculated) magnetic fields based on the 5-fitted dipole locations from Fig. 3b are plotted in Fig. 3d and the residual (the difference between the measured and predicted magnetic fields) is plotted in Fig. 3e.
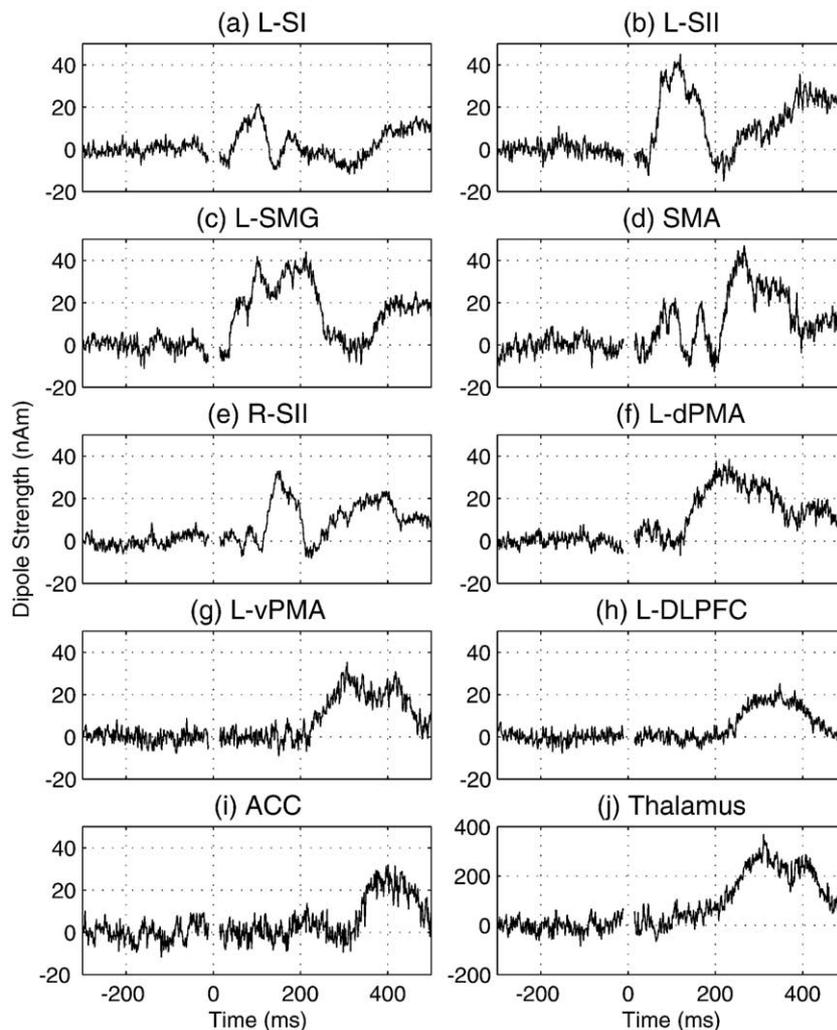

Fig. 5. Dipole time-courses for the 10 sources during the 15–500 ms interval from the same representative subject's right arm median-nerve oddball responses (rare minus frequent stimuli). (a) Left SI. (b) Left SII. (c) Left SMG. (d) Midline SMA. (e) Right SII. (f) Left dPMA. (g) Left vPMA. (h) Left DLPFC. (i) Midline ACC. (j) Left thalamus. Baseline noise for the −300 to −10 ms pre-stimulus interval is also shown for each source.

The small residual confirms the goodness-of-fit to the data resulting from the MSST calculation of neuronal sources.

The same process was performed for the other two intervals (150–250 ms and 250–500 ms). For this subject's responses evoked by right median-nerve oddball stimulation, 10 non-redundant sources were localized in the rare minus frequent responses for the 15–500 ms interval (Fig. 4a). A Monte-Carlo analysis (Medvick et al., 1989) was used to provide the statistical uncertainty of the dipole solutions from MSST. The red clusters in Fig. 4 show the uncertainty (3 standard-deviation range) of the 10 localized dipoles, superimposed onto this subject's MRI. These sources are: left (contralateral) SI, SII, SMG, dPMA, DLPFC, ventral premotor area (vPMA), thalamus, midline SMA, ACC, and right (ipsilateral) SII. Note that unlike fMRI activation images, a large cluster indicates large localization uncertainty, which usually suggests a distributed or weak source. Five of these 10 sources, namely left SI, SII, SMG, midline SMA, and right SII, showed activation during the first 15–150 ms interval, corresponding to the location plot in Fig. 3b. In this subject, the right SII ipsilateral to the stimulation was slightly superior to the contralateral (left) SII source. We believe that this location difference may be due to a weak ipsilateral SI activation that co-exists with the ipsilateral SII source in a small portion of subjects (Kanno et al., 2003).

For comparison, neuronal generators driving the MEG responses evoked by frequent median-nerve stimulation to the right arm of the subject were also localized, following the same procedure used for analyzing difference (rare minus frequent) responses. The locations of these sources, shown in Fig. 4b, were in left SI, left M1, midline SMA, right SII, and left SII areas. The relatively small uncertainty in the locations of sources is likely due to the lower noise level associated with the large number of trials that contributed to the average. These sources have been routinely localized by many groups (including ours) using traditional (non-oddball) median-nerve stimulation tasks: (1) SI (Wood et al., 1985; Hari et al., 1993; Forss et al., 1994; Mauguiere et al., 1997a,b; Forss and Jousmaki, 1998; Jousmaki and Forss, 1998; Hari and Forss, 1999); (2) M1 (Baldissera and Leocani, 1995; Kawamura et al., 1996; Spiegel et al., 1999; Huang et al., 2004a,b; Balzamo et al., 2004); (3) SMA (Urbano et al., 1997; Boakye et al., 2000; Barba et al., 2001); and (4) bilateral SIIs (Hari et al., 1993; Forss and Jousmaki, 1998; Hari and Forss, 1999; Fujiwara et al., 2002; Simoes et al., 2003).

Responses to rare stimuli were more difficult to model, since they contained a large number of generators including activations that were modulated by selective attention and others that were not (e.g., M20 and M30). The novel oddball design in the present study allowed direct subtraction of the frequent responses from the rare responses, thus greatly increasing the reliability of localizing selective attention-related brain activation. For this reason, the remaining analyses focus on the rare minus frequent oddball responses.

Fig. 5 shows the individual dipole time-courses (rare minus frequent stimuli) for the 10 right-arm oddball evoked sources during the 15–500 ms interval in the same subject. Baseline noise levels for these sources are also shown. The baselines were obtained by fitting the −300 to −10 ms interval with the same dipole location parameters used for fitting the 15–300 ms interval. The −10 to 15 ms interval was not included in the fit to avoid potential contamination from the stimulation artifact. Four sources showed robust activation before 100 ms: left SI (Fig. 5a), SII (Fig. 5b), IPL/SMG (Fig. 5c), and midline SMA (Fig. 5d). The dominant

generator is the left SII source with its first peak at about 75 ms, followed by a second peak at about 110 ms. In contrast, the IPL/SMG source shows its first peak at about 50 ms.

The main peak of the right (ipsilateral) SII was at about 150 ms (Fig. 5e), much later than the left (contralateral) SII. The left dPMA source showed a peak at about 200 ms (Fig. 5f). The time-course of SMA showed three peaks at about 100 ms, 150 ms, and 250 ms. The left vPMA time-course showed no early activation, with its first peak at about 300 ms (Fig. 5g). Importantly, both left DLPFC and ACC, the frontal components of the parietal–frontal network, also showed later peak latencies between 300 and 400 ms (Fig. 5h, i). Similarly, the left thalamus source peak activation occurred between 300 and 400 ms (Fig. 5j). Note that the thalamus dipole strength is large (i.e., the vertical scale is about 10 times higher than the others), which is essential in order for MEG to localize a deep source (Hämäläinen and Sarvas, 1989).

Talairach coordinates of the averaged source-locations for the group

For the entire group of 9 subjects, we first performed group-analyses for the dipole locations. Table 1 lists the mean and SD of

Table 1
Talairach coordinates (mean ± standard deviation) of major sources across subjects during the 15–500 ms interval[a]

Source (total:R:L)[b]	x (mm)	y (mm)	z (mm)
SI			
L (10:7:3)	−34.9 ± 6.4	−31.5 ± 9.4	56.0 ± 6.8
R (9:2:7)	37.6 ± 10.7	−30.6 ± 5.8	54.8 ± 9.0
SII			
L (16:9:7)	−49.3 ± 3.1	−17.3 ± 7.5*	20.6 ± 8.1
R (16:7:9)	50.4 ± 5.0	−10.5 ± 8.7*	26.0 ± 7.7
IPL/SMG			
L (10:9:1)	−37.5 ± 3.3**	50.2 ± 7.7	46.0 ± 6.2
R (7:0:7)	46.1 ± 6.4**	46.6 ± 7.8	41.3 ± 5.8
dPMA/M1			
L (9:8:1)	−31.9 ± 7.1	−19.1 ± 5.5*	55.3 ± 6.0
R (10:3:7)	36.6 ± 4.2	−14.0 ± 4.7*	54.8 ± 7.4
DLPFC/MFG			
L (10:5:5)	−34.7 ± 8.7	25.7 ± 9.2	29.5 ± 12.6
R (10:3:7)	37.5 ± 6.1	23.8 ± 12.6	30.4 ± 16.2
VPMA			
L (6:5:1)	−46.0 ± 7.6	1.4 ± 7.8	25.9 ± 6.6
R (5:0:5)	48.9 ± 5.6	6.1 ± 3.8	24.7 ± 6.5
Thalamus			
L (5:5:0)	−11.2 ± 3.8	−7.8 ± 6.1	7.8 ± 3.2
R (7:0:7)	11.8 ± 6.4	−5.9 ± 5.3	7.1 ± 4.4
SMA			
Midline (13:8:5)	−0.7 ± 8.5	−17.2 ± 7.5	61.2 ± 7.5
ACC			
Midline (13:6:7)	0.6 ± 6.9	25.2 ± 17.9	35.7 ± 13.5

9 subjects 18 hemispheres. Asterisks signify x, y, z coordinates that were significantly different between the hemispheres.

[a] The calculations for the mean and standard deviation of each x, y, z coordinate were based on the total number of responses, irrespective of the side of stimulation.

[b] The numbers in the parentheses following each source are: the total number of sources evoked by stimulation of either right or left median-nerve, only right median-nerve, and only left median-nerve (rare minus frequent) stimulation.

* $P < 0.05$.

** $P < 0.01$.

the Talairach coordinates for the major MEG sources (sources that were localizable in more than 30% of the responses) averaged across all subjects for the entire 15–500 ms interval (rare minus frequent). The majority of sources were evoked by the contralateral median-nerve oddball (rare minus frequent) stimulation, although some were evoked by ipsilateral stimulation as well. A few sources showed significant hemispheric asymmetry in their spatial location. First, left SII was significantly posterior to the right SII ($t = 2.38$, $P < 0.05$, $df = 30$, two-tailed). The left SII also showed a non-significant trend of being inferior (ventral) to right SII ($t = 1.95$, $P = 0.0611$, $df = 30$). Second, left IPL/SMG was significantly medial to the right IPL/SMG ($t = 3.63$, $P < 0.01$, $df = 15$). Third, the left dPMA/M1 was significantly posterior to the right dPMA/M1 ($t = 2.19$, $P < 0.05$, $df = 17$). A non-significant trend was also observed for the left dPMA/M1 to be more medial than the right dPMA/M1 ($t = 1.78$, $P = 0.0931$, $df = 17$).

Although the mean coordinates of ACC and DLPFC dipoles are in-line with the standard Talairach coordinates, relatively large standard deviations in the y and z coordinates for both ACC and DLPFC were observed, likely due to the spherical head model used in the analysis. Spherical head model is adequate for localizing sources along the central sulcus and in the parietal lobe, but less accurate for sources in the anterior portion of the frontal lobe (e.g., Huang et al., 1999) particularly affecting the obtained y and z coordinates of ACC and DLPFC dipoles.

Source time-courses averaged across subjects (Rare Minus Frequent Stimuli): onset latency and hemispheric differences

Fig. 6 shows the averaged dipole time-courses across all subjects for major cortical sources during the 15–500 ms interval computed from difference waveforms (rare minus frequent). Zero activation was assumed if a source was missing in a subject's response during the group averaging. The error bars indicate the standard deviations of the dipole time-courses. Error bars are drawn for representative latencies. The information regarding side of stimulation is provided for each source because time-courses differed for contralateral and ipsilateral activity.
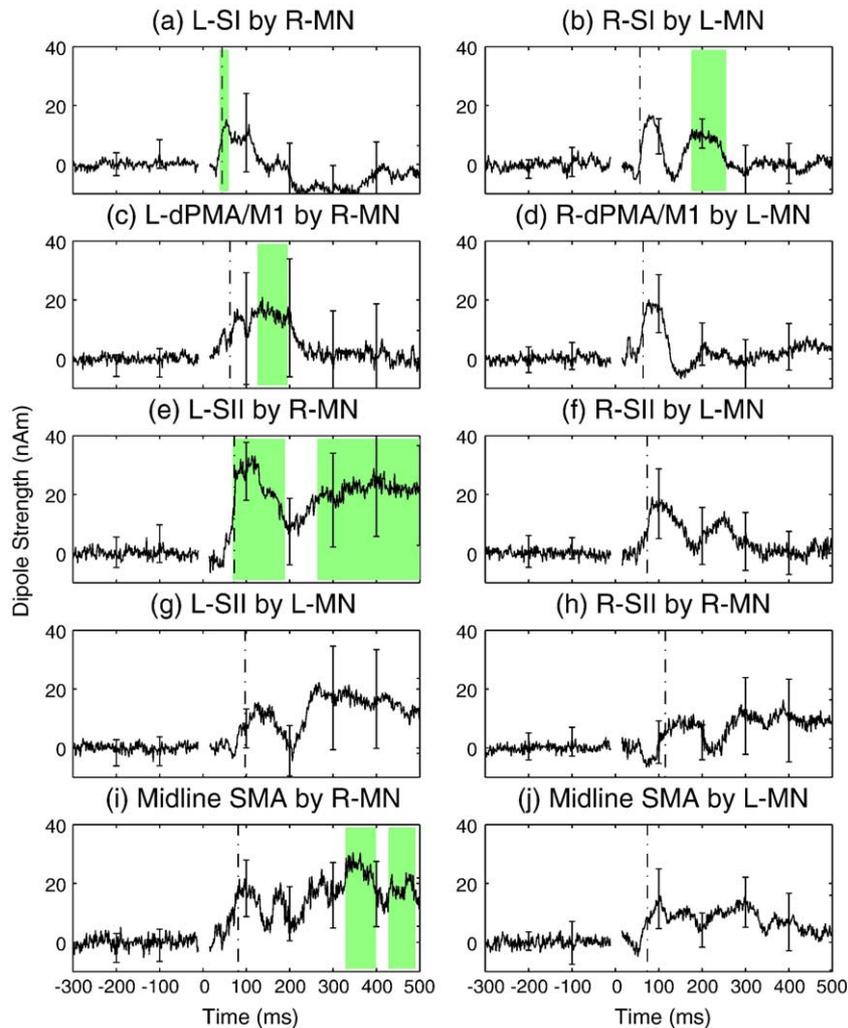

Fig. 6. Group-averaged dipole time-courses for major cortical sources of oddball responses during the 15–500 ms interval (rare minus frequent stimuli). Error bars indicate the standard deviations of time-courses for the 100, 200, 300, 400, and 500 ms latencies. The shaded area(s) designate epochs in which the dipole amplitude of a source was significantly stronger ($P < 0.05$) in one hemisphere than the other (i.e., the figure on opposite side) for the same time interval. The vertical dash-dotted line in each plot designates the mean onset latency of the earliest major peak for a source. The mean and SD of baseline noise for the −300 to −10 ms pre-stimulus interval is also shown for each source.
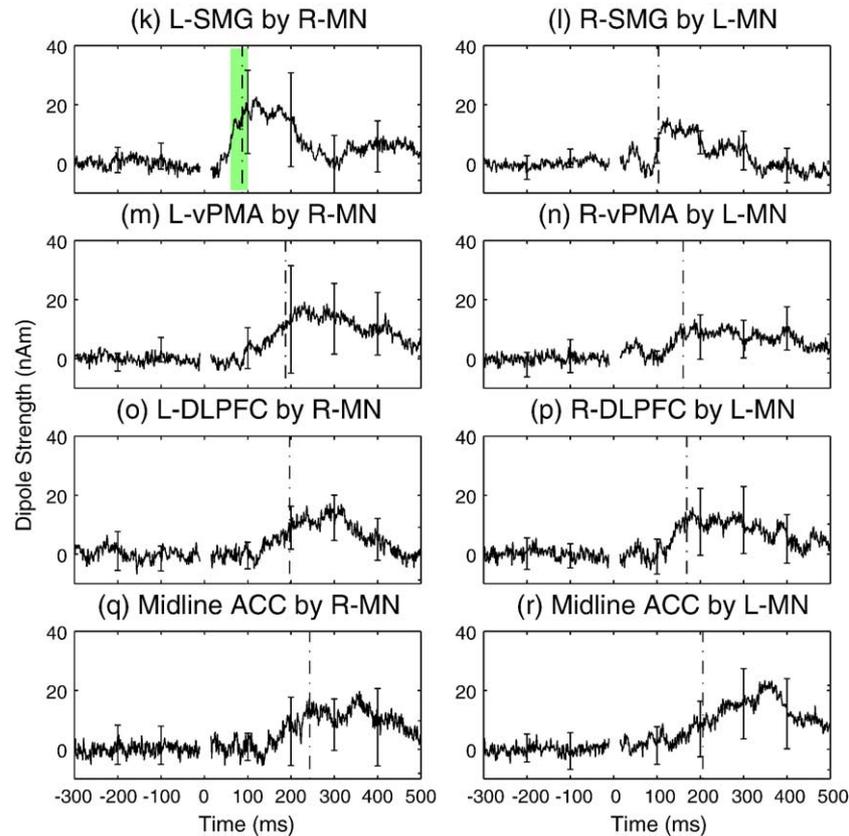
Fig. 6 (*continued*).

First, we focused on the hemispheric asymmetry of the dipole amplitude for the same source across different hemispheres. The shaded area(s) designate epochs during which dipole amplitude was significantly stronger ($P < 0.05$) than the homologous dipole in the other hemisphere for the same time interval. Most of these comparisons demonstrated that dipole strength in the left hemisphere was greater than in the right hemisphere. For example, Fig. 6a shows the averaged dipole time-course from the left SI source evoked by right (contralateral) median-nerve oddball stimulation. The shaded area in Fig. 6a 38–59 ms indicates that the left contralateral SI source was significantly stronger than the right contralateral SI source (Fig. 6b). Similarly, the left contralateral dPMA/M1 (Fig. 6c) was significantly stronger than the right contralateral dPMA/M1 (Fig. 6d) during the 126–195 ms interval. The strongest hemispheric asymmetry was seen in contralateral SII, wherein the left contralateral SII (Fig. 6e) was stronger than the right contralateral SII (Fig. 6f) during the 69–189 ms and the 264–500 ms epochs. The SMA response evoked by right-sided stimulation (Fig. 6i) was stronger than the SMA response evoked by left-sided stimulation (Fig. 6j) during the 329–399 ms and 428–490 ms epochs. The left contralateral SMG/IPL response (Fig. 6k) was also significantly stronger than the right contralateral SMG/IPL response (Fig. 6l) during the 61–100 ms interval. These left hemisphere biases contrasted with the right SI response evoked by left-sided stimulation (Fig. 6b), which was the only source in the right hemisphere showing significantly stronger activation than the corresponding source in the left hemisphere (Fig. 6a), but only during the 175–255 ms interval. Fig. 6 shows that hemispheric asymmetry was not found for ipsilateral SII sources (g, h),

contralateral vPMA (m, n) and DLPFC (o, p) sources, or ACC sources.

The conventional 0.05 p-level was adopted due to the exploratory nature of these comparisons using time-point-by-time-point t tests. Because multiple t tests may increase Type I errors, we also performed a single t test for area-under-curve (AUC) of the shaded areas in Fig. 6. The P values of the AUC for the intervals in the shaded areas in Fig. 6 were all less than 0.05, which confirmed our findings without encountering the multiple t test issue.

Next, we examined whether there were within-hemispheric onset latency differences among the sources. The vertical dash-dotted line in each plot of Fig. 6 designates the mean onset latency of the earliest major peak for a source, averaged across subjects. The onset latency of each source time-course from an individual subject was defined as the time corresponding to the half-maximum-amplitude of the earliest major peak. The mean onset latencies are listed in Table 2. t tests compared the onset latency of each source within a hemisphere.

Within the left hemisphere (A1–A9 in Table 2), the onset latency of the left contralateral SI source (44.0 ms) was significantly earlier than all other left hemisphere sources except contralateral dPMA/M1. The left contralateral dPMA/M1 source had the second earliest onset latency (62.4 ms), which was significantly earlier than onset latencies in ipsilateral SII, ACC, and contralateral SMG, vPMA, and DLPFC. Left contralateral SII had the third earliest onset latency (72.3 ms), which was significantly earlier than the left ipsilateral SII, the ACC, and the contralateral vPMA and DLPFC. Next, mean onset latency of the SMA evoked by right median-nerve oddball stimulation (80.9 ms)

Table 2
Mean (±standard deviation) onset latencies of major cortical sources across all subjects

Source (subjects)/stimulation side	Onset latency (ms)	A1	A2	A3	A4	A5	A6	A7	A8	A9
A1: L-SI(7)/R	44.0 ± 13.6		n.s.	***	**	*	***	***	***	***
A2: L-dPMA-M1(8)/R	62.4 ± 34.6			n.s.	n.s.	n.s.	*	***	***	***
A3: L-SII(9)/R	72.3 ± 12.4				n.s.	n.s.	**	***	***	***
A4: SMA(8)/R	80.9 ± 27.3					n.s.	n.s.	***	***	***
A5: L-SMG(9)/R	87.3 ± 39.0						n.s.	**	***	***
A6: L-SII(7)/L	96.9 ± 18.1							**	***	***
A7: L-vPMA(5)/R	187.2 ± 49.3								n.s.	n.s.
A8: L-DLPFC(5)/R	197.0 ± 36.9									n.s.
A9: ACC(6)/R	243.2 ± 61.4									

Source (subjects)/stimulation side	Onset latency (ms)	B1	B2	B3	B4	B5	B6	B7	B8	B9
B1: R-SI(7)/L	56.9 ± 11.6		n.s.	*	*	***	***	***	***	***
B2: R-dPMA-M1(7)/L	63.9 ± 13.8			n.s.	n.s.	n.s.	***	***	***	***
B3: R-SII(9)/L	73.1 ± 14.2				n.s.	***	***	***	***	***
B4: SMA(5)/L	73.8 ± 13.4					**	**	**	**	**
B5: R-SMG(7)/L	103.6 ± 12.3						n.s.	*	**	**
B6: R-SII(7)/R	115.4 ± 16.9							*	*	**
B7: R-vPMA(5)/L	160.2 ± 46.3								n.s.	n.s.
B8: R-DLPFC(7)/L	168.6 ± 44.9									n.s.
B9: ACC(7)/L	205.7 ± 66.2									

N = 9. A1–A9 are left hemispheric sources (including the midline SMA and ACC) which were evoked by right arm median-nerve stimulation (rare minus frequent). An exception is the ipsilateral left SII source (A6 in the Table), which was evoked by left arm median-nerve stimulation. B1–B9 are right hemispheric sources (including the midline SMA and ACC) evoked by left arm median-nerve stimulation. An exception is the ipsilateral right SII source (B6 in the Table) which was evoked by right arm median-nerve stimulation. The number in parentheses following the source name specifies the number of responses in which that source was localizable. Onset latency is based on the difference between rare and frequent median-nerve stimulation. Results of statistical analyses between the Sources A1–A9 and between Sources B10–B9 were shown in the upper-right sections. *$P < 0.05$, **$P < 0.01$, ***$P < 0.001$, n.s. not significant.

was significantly earlier than the ACC and the contralateral vPMA and DLPFC. The next left hemisphere source in sequence was contralateral SMG/IPL, which showed a significantly earlier onset latency (87.3 ms) than the ACC and the contralateral vPMA and DLPFC. Finally, the onset latency of left ipsilateral SII (96.9 ms) was significantly earlier than the contralateral vPMA and DLPFC, and the ACC. The last three sources in sequence were the left contralateral vPMA (187.2 ms), left contralateral DLPFC (197 ms), and ACC (243.2 ms), which did not differ significantly in their onset latencies.

Nearly identical results were found for the mean onset latencies among the sources in the right hemisphere (Sources B1–B9 in Table 2). The earliest source was right contralateral SI (56.9 ms), which significantly preceded all other sources except right contralateral dPMA/M1. The right contralateral dPMA/M1 source had the second earliest onset latency (63.9 ms), beginning significantly earlier than the ipsilateral SII, the contralateral vPMA and DLPFC, and the ACC. The contralateral SII had the third earliest onset latency (73.1 ms), beginning significantly earlier than ipsilateral SII, contralateral SMG/ILP, vPMA and DLPFC, and the ACC. The mean onset latency of the SMA evoked by left-sided stimulation (73.8 ms) was significantly earlier than contralateral SMG/IPL, vPMA, and DLPFC, and the ACC. The next right hemispheric source in sequence was the contralateral SMG/ILP, which was significantly earlier (103.6 ms) than contralateral vPMA and DLPFC and the ACC. The ipsilateral SII onset latency (115.4 ms) was also significantly earlier than contralateral vPMA and DLPFC, and the ACC. Finally, the last three sources in sequence were again the contralateral vPMA (160.2 ms) and DLPFC (168.6 ms) and the ACC (205.7 ms), which did not differ significantly in their onset latencies.

As for hemispheric asymmetry of the onset latency, no significant latency differences were found between any source in the right hemisphere and its corresponding source in the left hemisphere. There was also no latency difference between the midline SMA or ACC responses activated by left- and right-sided stimulation.

Discussion

The present results showed for the first time that the same parietal–frontal network known to be commonly activated by auditory and visual oddball stimuli is also robustly activated during a somatosensory oddball task. The locations of the activated areas (i.e., IPL/SMG, DLPFC/MFG, and ACC) in the parietal–frontal network were consistent with previous intracranial and fMRI studies using auditory and visual stimuli (Halgren et al., 1998; McCarthy et al., 1997; Menon et al., 1997; Linden et al., 1999; Yoshiura et al., 1999; Stevens et al., 2000; Clark et al., 2000; Kiehl and Liddle, 2001; Ardekani et al., 2002). These results together with present findings strengthen the evidence for a modality-independent parietal–frontal network that supports selective attention to novel events. The reason that IPL/SMG, ACC, and DLPFC/MFG in the present study are considered to be activated in a network fashion and not just coincidentally is that none of these areas is part of the standard somatosensory systems, and none shows activation in a somatosensory test not involving selective attention. The apparent modality-independence of activation in the IPL/SMG and the DLPFC/MFG may represent an important cortical network in early processing stages of working memory (Halgren et al., 1998; McCarthy et al., 1997). This is supported by

physiological studies in monkeys (Baddeley, 1992) and neuro-imaging studies in humans (Cohen et al., 1994; Smith et al., 1995; McCarthy et al., 1994, 1996), which reveal a similar neuronal network underlying cognitive operations involved in working memory. This working memory network involves reciprocal interconnections between the DLPFC, inferior parietal cortex, and other cortical, subcortical, and cerebellar structures (Goldman-Rakic, 1987, 1988; Mesulam, 1990).

The millisecond temporal resolution of MEG also uncovered the precise time-course of the activation within this parietal–frontal network. The onset latency of IPL/SMG activity was early in both hemispheres (87 ms and 104 ms in the left and right hemispheres, respectively), significantly preceding activity in the DLPFC/MFG by 65 ms to 110 ms and ACC by 102 ms to 156 ms (Table 2, Fig. 6). This finding is consistent with the relative time course of fMRI activity in parietal and DLPFC during the performance of auditory and visual oddball tasks (Stevens et al., 2000). This finding is also striking since it provides direct evidence that the IPL/SMG is involved in the early stage of the soma-tosensory oddball response. SMA and vPMA were also consis-tently activated during the median-nerve oddball task, which has been reported in fMRI studies using auditory and visual oddball stimuli (Yoshiura et al., 1999; Stevens et al., 2000; Ardekani et al., 2002). These studies, including our own, required subjects to silently count the rare stimuli without an overt motor response. For this reason, vPMA and SMA activations may be due to planning an unexecuted motor orienting response and represent a possible attentional role in sensory processing (Ardekani et al., 2002; Downar et al., 2000).

Many fMRI studies have also reported what appears to be modality-independent activation in the thalamus during oddball auditory tasks (Kiehl and Liddle, 2001; Menon et al., 1997), oddball visual tasks (Clark et al., 2000; Ardekani et al., 2002), or both auditory and visual tasks (Yoshiura et al., 1999). Similarly, Yingling and Hosobuchi (1984) examined a patient suffering from chronic refractory pain, who had a multi-contact electrode implanted in the ventro-postero-lateral nucleus (VPL). They observed a negative potential at latencies of 300–450 ms, which was selectively evoked by auditory and visual rare target stimuli detection. There have been some concerns as to whether thalamus activation can be observed using MEG due to the location of the thalamus deep within the brain. In the present study, the tight cluster in the thalamus derived from the Monte-Carlo analysis empirically demonstrates a small localization uncertainty, which indicates that this source is indeed reliably localized in the representative subject (Fig. 3). Across subjects (Table 1), we observed thalamus activation in 67% of the 18 median-nerve oddball responses in our 9 subjects, further supporting the credibility of this source. Still, no firm conclusions can be drawn regarding the time-course of the thalamic activation in our study, because calculations of dipole moments of deep sources by MEG are less reliable than calculating the location and amplitude of such deep sources.

In addition to modality-independent areas, the present results also identified regions (i.e., bilateral SIIs, SI, and dPMA/M1) that are uniquely related to processing somatosensory oddball responses. The contralateral SI and bilateral SII activations demonstrate that both the primary and secondary somatosensory areas are sensitive to attention-related median-nerve oddball stimulation, which is consistent with previous findings (Mima et al., 1998; Fujiwara et al., 2002). Moreover, contralateral SII was

the only source localized in all 18 responses across the 9 subjects (Table 1), which illustrates this region's crucial role in processing oddball information in the somatosensory system. Our MEG results also showed that in both hemispheres, the onset latencies of all somatosensory-specific sources were significantly earlier than the frontal component of the parietal–frontal network (i.e., DLPFC/MFG and ACC). Only activity in contralateral SI and contralateral SII (right hemisphere) significantly preceded activity in the parietal component of the network (IPL/SMG). These findings demonstrate a trend for somatosensory processing to flow from the posterior to the anterior cortices.

We also found robust activation in dPMA/M1, which has not been reported previously. It is possible that previous MEG somatosensory oddball studies under-modeled the data and the activation from dPMA/M1 (and other areas) was modeled in combination with the SI source. Another difference between the current study and previous studies was the use of the difference-response (rare minus frequent stimuli) in our data analysis, which removed the non-oddball related responses (e.g., the strong and sharp N20 m and P30 m components) and allowed us to focus directly on the oddball-induced changes. This was possible because stimulus parameters in our novel oddball design were identical between rare and frequent stimuli, and the only difference was the subject's focus of attention. Consequently, the difference waveform allowed us to reliably localize sources such as dPMA/M1, which are difficult to identify in traditional oddball paradigms.

Our study also found inter-hemispheric location asymmetry in SII, dPMA/M1, and IPL/SMG. Inter-hemispheric asymmetry of various sources has been well documented in the somatosensory system using MEG recordings during the performance of tasks other than the oddball paradigm. In the standard median-nerve stimulation task, Wikström et al. (1997) reported that the generators of N20 m, P35 m, and P60 m in the left hemisphere were significantly medial to their counter sources in the right hemisphere. In addition, N20 m and P60 m sources in the left hemisphere were located significantly posterior to those in the right hemisphere. Using tactile somato-sensory stimulation, Reite et al. (2003) also reported that the SI generator in the left hemisphere was located significantly posterior to the right SI. Interestingly, they found that patients with schizophrenia showed reduced asymmetry for this source. Although our findings are generally consistent with the idea that left hemisphere sources during somatosensory stimulation are situated medial and posterior to those in the right hemisphere, there are still some discrepancies between our study and previous studies. First, we found only a nonsignificant trend for left SI to be medial and posterior to the right SI. This may be due to our smaller sample size ($n = 9$) relative to previous MEG studies ($n = 23$ in Wikström et al., 1997; $n = 15$ in Reite et al., 2003). Second, we found that left SII was located more posterior to right SII, whereas this was not shown in another MEG study (Wikström et al., 1997). This discrepancy may due to our strong dominant SII responses evoked by the oddball paradigm, which would increase the likelihood of accurately localizing this source. Indeed, Wikström et al. (1997) themselves speculated that the low SNR in their standard median-nerve paradigm may have contributed to the absence of hemispheric asymmetry in SII.

We also found inter-hemispheric asymmetry in the dipole amplitude for contralateral SI, contralateral SII, contralateral dPMA/M1, and contralateral SMG/IPL, which generally was significantly stronger in the left than the right hemisphere (Fig. 6). Such asymmetries may be explained by left hemisphere

dominance in our right-handed subjects, although this has not been reported by previous studies using somatosensory oddball tests.

In the present study, all 850 trials in the frequent condition and 150 trials in the rare condition were used in the signal averaging. To take an equal number of trials for both the rare and frequent conditions, we would have to exclude a large number of frequent trials. In practice, it would be difficult to come with an objective criterion for including certain frequent trials while excluding other frequent trials. One could select trials at random, but that does not necessarily rule out the possibility of unequal SDs between conditions. More importantly, with the emphasis in the present case on analysis of difference waveforms, the difference in number of available trials does not play out in the same way. If we were to limit ourselves to the same number of trials (150) in both conditions, the noise standard deviation in the rare-minus-frequent waveform would be 1.41 (i.e., $\sqrt{2}$) times the noise standard deviation in either condition, because variances for difference scores are additive. Such a 41% increase of the noise standard deviation would cause concern. Instead, by using all 850 frequent trials and 150 rare trials, the noise standard deviation in the rare-minus-frequent waveform is just 1.08 (i.e., $\sqrt{(1 + 150/850)}$) times the noise standard deviation of the waveform in the rare condition, an increase of only 8%. This advantage in noise level can be easily seen in Fig. 2, in which the noise level in the averaged difference waveform was quite similar to that in the rare condition.

As a final comment, we did not consistently observe hippocampal activation during selective attention to somatosensory stimulation. A hippocampal source was identified in only five cases (three right and two left hemisphere sources). This contrasts with hippocampal activation in intracranial recordings during auditory and visual oddball tests (e.g., Halgren et al., 1995b). We believe that the absence of reliable hippocampal activation in our study may be due to the strong SII cortical activation, which can reduce the sensitivity of MEG for localizing deep sources beneath the SII.

In conclusion, the present results showed that the somatosensory oddball median-nerve stimuli task activates the same parietal–frontal network as auditory and visual oddball tests have in previous studies. The key cortical areas involved in this parietal–frontal network are IPL/SMG, ACC, and DLPFC/MFG. The activation in the IPL/SMG area markedly preceded activations in the frontal cortex, suggesting they play a role in early attention processes that are integrally linked with working memory. We also identified areas that are uniquely related (modality specific) to somatosensory oddball responses including the bilateral SII, SI, dPMA, M1, and SMA. The knowledge gained from the present study may be useful as a normative baseline for exploring somatosensory deficits in patients with neurological and psychiatric disorders (Huang et al., in preparation).

Acknowledgments

References

Aine, C., Huang, M., Stephen, J., Christner, R., 2000. Multi-start algorithms for MEG empirical data analysis reliably characterize locations and time-courses of multiple sources. NeuroImage 12, 159–172.

Allison, T., Wood, C.C., McCarthy, G., Spencer, D.D., 1991a. Cortical somatosensory evoked potentials. II. Effects of excision of somatosensory or motor cortex in humans and monkeys. J. Neurophysiol. 66, 64–82.

Allison, T., McCarthy, G., Wood, C.C., Jones, S.J., 1991b. Potentials evoked in human and monkey cerebral cortex by stimulation of the median nerve. Brain 114, 2465–2503.

Anderer, P., Pascual-Marqui, R.D., Semlitsch, H.V., Saletu, B., 1998. Differential effects of normal aging on sources of standard N1, target N1 and target P300 auditory event-related brain potentials revealed by low resolution electromagnetic tomography (LORETA). Electroencephalogr. Clin. Neurophysiol. 108, 160–174.

Ardekani, B.A., Choi, S.J., Hossein-Zadeh, G.A., Porjesz, B., Tanabe, J.L., Lim, K.O., Bilder, R., Helpern, J.A., Begleiter, H., 2002. Functional magnetic resonance imaging of brain activity in the visual oddball task. Cogn. Brain Res. 14 (3), 347–356.

Asanuma, H., Larsen, K.D., Yumiya, H., 1980. Peripheral input pathways to the monkey motor cortex. Exp. Brain Res. 38, 349–355.

Ashburner, J., Friston, K.J., 1999. Nonlinear spatial normalization using basis functions. Hum. Brain Mapp. 7 (4), 254–266.

Ashburner, J., Neelin, P., Collins, D.L., Evans, A.C., Friston, K.J., 1997. Incorporating prior knowledge into image registration. NeuroImage 6, 344–352.

Baddeley, A., 1992. Working memory. Science 255, 556–559.

Baldissera, F., Leocani, L., 1995. Afferent excitation of human motor cortex as revealed by enhancement of direct cortico-spinal action on motoneurones. Electroencephalogr. Clin. Neurophysiol. 97, 394–401.

Balzamo, E., Marquis, P., Chauvel, P., Regis, J., 2004. Short-latency components of evoked potentials to median nerve stimulation recorded by intracerebral electrodes in the human pre- and postcentral areas. Clin. Neurophysiol. 115 (7), 1616–1623.

Barba, C., Frot, M., Guenot, M., Mauguiere, F., 2001. Stereotactic recordings of median nerve somatosensory-evoked potentials in the human pre-supplementary motor area. Eur. J. Neurosci. 13 (2), 347–356.

Baudena, P., Halgren, E., Heit, G., Clarke, J.M., 1995. Intracerebral potentials to rare target and distractor auditory and visual stimuli: III. Frontal cortex. Electroencephalogr. Clin. Neurophysiol. 94, 251–264.

Berg, P., Scherg, M., 1994. Handbook of BESA: Brain Electric Source Analysis, Version 2.0. MEGIS, Munich.

Boakye, M., Huckins, S.C., Szeverenyi, N.M., Taskey, B.I., Hodge Jr., C.J., 2000. Functional magnetic resonance imaging of somatosensory cortex activity produced by electrical stimulation of the median nerve or tactile stimulation of the index finger. J. Neurosurg. 93 (5), 774–783.

Clark, V.P., Fannon, S., Lai, S., Benson, R., Bauer, L., 2000. Responses to rare visual target and distractor stimuli using event-related fMRI. J. Neurophysiol. 83 (5), 3133–3139.

Cohen, J.D., Forman, S.D., Braver, T.S., Casey, B.J., Servan-Schreiber, D., Noll, D.C., 1994. Activation of prefrontal cortex in a non-spatial working memory task with functional MRI. Hum. Brain Map. 1, 293–304.

Davidoff, R.A., 1990. The pyramidal tract. Neurology 40, 332–339.

De Munck, J.C., 1990. The estimation time varying on the basis of evoked potentials. Electroencephalogr. Clin. Neurophysiol. 77, 156–160.

Desmedt, J.E., Tomberg, C., 1989. Mapping early somatosensory evoked potentials in selective attention: critical evaluation of control conditions used for titrating by difference the cognitive P30, P40, P100 and N140. Electroencephalogr. Clin. Neurophysiol. 74 (5), 321–346.

Downar, J., Crawley, A.P., Mikulis, D.J., Davis, K.D., 2000. A multimodal cortical network for the detection of changes in the sensory environment. Nat. Neurosci. 3 (3), 277–283.

Ferguson, A.S., Zhang, X., Stroink, G., 1994. A complete linear discretiza-

tion for calculating the magnetic field using the boundary element method. IEEE. Trans. Biomed. Eng. 41, 455–459.

Forss, N., Jousmaki, V., 1998. Sensorimotor integration in human primary and secondary somatosensory cortices. Brain Res. 781 (1–2), 259–267.

Forss, N., Hari, R., Salmelin, R., Ahonen, A., Hamalainen, M., Kajola, M., Knuutila, J., Simola, J., 1994. Activation of the human posterior parietal cortex by median nerve stimulation. Exp. Brain. Res. 99 (2), 309–315.

Friston, K.J., Ashburner, J., Frith, C.D., Poline, J.-B., Heather, J.D., Frackowiak, R.S.J., 1995. Spatial registration and normalization of images. Hum. Brain Mapp. 2, 165–189.

Fujiwara, N., Imai, M., Nagamine, T., Mima, T., Oga, T., Takeshita, K., Toma, K., Shibasaki, H., 2002. Second somatosensory area (SII) plays a significant role in selective somatosensory attention. Brain Res. Cogn. Brain Res. 14 (3), 389–397.

Garcia-Larrea, L., Lukaszewicz, A.C., Mauguiere, F., 1995. Somatosensory responses during selective spatial attention: the N120-to-N140 transition. Psychophysiology 32 (6), 526–537.

Goldman-Rakic, P.S., 1987. Circuitry of primate prefrontal cortex and regulation of behavior by representational memory. The Nervous System. Higher Functions of the Brain, Handbook of Physiology, vol. V. American Physiological Society, Bethesda, MD, pp. 373–417.Sect. 1.

Goldman-Rakic, P.S., 1988. Topography of cognition: parallel distributed networks in primate association cortex. Annu. Rev. Neurosci. 11, 137–156.

Golub, G.H., Van Loan, C.F., 1984. Matrix Computations, second edition John Hopkins Univ. Press.

Halgren, E., Squries, N.K., Wilson, C.L., Rohrbaugh, J.W., Babb, T.L., Crandall, P.H., 1980. Endogenous potential generated in the human hippocampal formation and amygdala by infrequent events. Science 210, 803–805.

Halgren, E., Baudena, P., Clarke, J.M., Heit, G., Liegeois, C., Chauvel, P., Musolino, A., 1995a. Intracerebral potentials to rare target and distractor auditory and visual stimuli: I. Superior temporal plane and parietal lobe. Electroencephalogr. Clin. Neurophysiol. 94, 191–220.

Halgren, E., Baudena, P., Clarke, J.M., Heit, G., Marinkovic, K., Devaux, B., Vignal, J.P., Biraben, A., 1995b. Intracerebral potentials to rare target and distractor auditory and visual stimuli: II. Medial, lateral and posterior temporal lobe. Electroencephalogr. Clin. Neurophysiol. 94, 229–250.

Halgren, E., Marinkovic, K., Chauvel, P., 1998. Generators of the late cognitive potentials in auditory and visual oddball tasks. Electroencephalogr. Clin. Neurophysiol. 106 (2), 156–164.

Hämäläinen, M.S., Sarvas, J., 1989. Realistic conductor geometry model of the human head for interpretation of neuromagnetic data. IEEE. Trans. Biomed. Eng. 36, 165–171.

Hanlon, F.M., Weisend, M.P., Huang, M., Lee, R.R., Moses, S.N., Paulson, K.M., Thoma, R.J., Miller, G.A., Canive, J.M., 2003. A non-invasive method for observing hippocampal function. NeuroReport 14 (15), 1957–1960.

Hansen, P.C., 1997. Rank-Deficit and Discrete Ill-Posed Problems: Numerical Aspects of Linear Inversion. SIAM, Philadelphia, PA.

Hari, R., Forss, N., 1999. Magnetoencephalography in the study of human somatosensory cortical processing. Philos. Trans. R. Soc. Lond., B Biol. Sci. 354 (1387), 1145–1154.

Hari, R., Hamalainen, H., Hamalainen, M., Kekoni, J., Sams, M., Tiihonen, J., 1990. Separate finger representations at the human second somatosensory cortex. Neuroscience 37 (1), 245–249.

Hari, R., Karhu, J., Hämäläinen, M., Knuutila, J., Salonen, O., Sams, M., Vilkman, V., 1993. Functional organization of the human first and second somatosensory cortices: a neuromagnetic study. Eur. J. Neurosci. 5 (6), 724–734.

He, B., Lian, J., Spencer, K.M., Dien, J., Donchin, E., 2001. A cortical potential imaging analysis of the P300 and novelty P3 components. Hum. Brain Mapp. 12, 120–130.

Hegerl, U., Frodl-Bauch, T., 1997. Dipole source analysis of P300

component of the auditory evoked potential: a methodological advance? Psychiatry Res. 74, 109–118.

Huang, M., Aine, C.J., Supek, S., Best, E., Ranken, D., Flynn, E.R., 1998. Multi-start downhill simplex method for spatio-temporal source localization in magnetoencephalography. Electroencephalogr. Clin. Neurophysiol. 108 (1), 32–44.

Huang, M.X., Mosher, J.C., Leahy, R.M., 1999. A sensor-weighted overlapping-sphere head model and exhaustive head model comparison for MEG. Phys. Med. Biol. 44 (2), 423–440.

Huang, M., Aine, C., Davis, L., Butman, J., Christner, R., Weisend, W., Stephen, J., Meyer, J., Silveri, J., Herman, M., Lee, R.R., 2000. Sources on the anterior and posterior banks of the central sulcus identified from magnetic somatosensory evoked responses using multi-start spatio-temporal localization. Hum. Brain Mapp. 11 (2), 59–76.

Huang, M., Davis, L.E., Aine, C., Weisend, M., Harrington, D., Christner, R., Stephen, J., Edgar, J.C., Herman, M., Meyer, J., Paulson, K., Martin, K., Lee, R.R., 2004a. MEG response to median nerve stimulation correlates with recovery of sensory and motor function after stroke. Clin. Neurophysiol. 115 (4), 820–833.

Huang, M., Harrington, D., Paulson, K., Weisend, M., Lee, R., 2004b. Temporal dynamics of ipsilateral and contralateral motor activity during voluntary finger movement. Hum. Brain Mapp. 23 (1), 26–39.

Jenkins, W.M., Merzenich, M.M., 1987. Reorganization of neo-cortical representations after brain injury: a neurophysiological model of the bases of recovery from stroke. Prog. Brain Res. 71, 249–266.

Johnson, R., Fedio, P., 1987. Task-related changes in P300 scalp distribution in temporal lobectomy patients. Electroencephalogr. Clin. Neurophysiol., Suppl. 40, 699–704.

Jones, E.G., Coulter, J.D., Hendry, S.H.C., 1978. Intracortical connectivity of architectonic field in somatic sensory, motor and parietalcortex of monkey. J. Comp. Neurol. 181, 291–348.

Jones, E.G., Wise, S.P., Coulter, J.D., 1979. Differential thalamic relationships of sensory-motor and parietal cortical fields in monkeys. J. Comp. Neurol. 183, 833–892.

Jousmaki, V., Forss, N., 1998. Effect of stimulus intensity on signals from human somatosensory cortices. NeuroReport 9 (15), 3427–3431.

Kanno, A., Nakasato, N., Hatanaka, K., Yoshimoto, T., 2003. Ipsilateral area 3b responses to median nerve somatosensory stimulation. NeuroImage 18 (1), 169–177.

Kawamura, T., Nakasato, N., Seki, K., Kanno, A., Fujita, S., Fujiwara, S., Yoshimoto, T., 1996. Neuromagnetic evidence of pre- and post-central cortical sources of somatosensory evoked responses. Electroencephalogr. Clin. Neurophysiol. 100, 44–50.

Kekoni, J., Hamalainen, H., McCloud, V., Reinikainen, K., Naatanen, R., 1996. Is the somatosensory N250 related to deviance discrimination or conscious target detection? Electroencephalogr. Clin. Neurophysiol. 100 (2), 115–125.

Kiehl, K.A., Liddle, P.F., 2001. An event-related functional magnetic resonance imaging study of an auditory oddball task in schizophrenia. Schizophr. Res. 48 (2–3), 159–171.

Kiss, I., Dashieff, R.M., Lordeon, P., 1989. A parieto-occipital generator for P300: evidence from human intracranial recordings. Int. J. Neurosci. 49, 133–139.

Knight, R.T., Scabini, D., Woods, D.L., Clayworth, C.C., 1989. Contributions of temporal–parietal junction to human auditory P3. Brain Res. 502, 109–116.

Knösche, T.R., Berends, E.M., Jagers, H.R.A., Peters, M.J., 1998. Determining the number of independent sources of the EEG: a simulation study on information criteria. Brain Topogr. 11, 111–124.

Leahy, R.M., Mosher, J.C., Spencer, M.E., Huang, M.X., Lewine, J.D., 1998. A study of dipole localization accuracy for MEG and EEG using a human skull phantom. Electroencephalogr. Clin. Neurophysiol. 107, 159–173.

Lemon, R.N., 1981. Functional properties of monkey motor cortex neurones receiving afferent input from the hand and fingers. J. Physiol. (London) 311, 497–519.

Lemon, R.N., Porter, R., 1976. Afferent input to movement-related

precentral neurones in conscious monkey. Proc. R. Soc. Lond. [Biol.] 194, 313–339.

Lemon, R.N., van der Burg, J., 1979. Short-latency peripheral inputs to thalamic neurones projecting to the motor cortex in the monkey. Exp. Brain Res. 36, 445–462.

Linden, D.E., Prvulovic, D., Formisano, E., Vollinger, M., Zanella, F.E., Goebel, R., Dierks, T., 1999. The functional neuroanatomy of target detection: an fMRI study of visual and auditory oddball tasks. Cereb. Cortex 9 (8), 815–823.

Lovrich, D., Novick, B., Vaughan, H.J., 1988. Topographic analysis of auditory event-related potentials associated with acoustic and semantic processing. Electroencephalogr. Clin. Neurophysiol. 71, 40–54.

Mauguiere, F., Merlet, I., Forss, N., Vanni, S., Jousmaki, V., Adeleine, P., Hari, R., 1997a. Activation of a distributed somatosensory cortical network in the human brain. A dipole modelling study of magnetic fields evoked by median nerve stimulation. Part I: location and activation timing of SEF sources. Electroencephalogr. Clin. Neurophysiol. 104 (4), 281–289.

Mauguiere, F., Merlet, I., Forss, N., Vanni, S., Jousmaki, V., Adeleine, P., Hari, R., 1997b. Activation of a distributed somatosensory cortical network in the human brain: a dipole modelling study of magnetic fields evoked by median nerve stimulation. Part II: effects of stimulus rate, attention and stimulus detection. Electroencephalogr. Clin. Neurophysiol. 104 (4), 290–295.

McCarthy, G., Wood, C.C., 1987. Intracranial recordings of endogenous ERPs in human. Electroencephalogr. Clin. Neurophysiol., Suppl. 39, 331–337.

McCarthy, G., Blamire, A.M., Puce, A., Nobre, A.C., Bloch, G., Hyder, F., Goldman-Rakic, P., Shulman, R.G., 1994. Functional MR imaging of human prefrontal cortex activation during a spatial working memory task. Proc. Natl. Acad. Sci. U. S. A. 91, 8690–8694.

McCarthy, G., Puce, A., Constable, R.T., Krystal, J.H., Gore, J.C., Goldman-Rakic, P., 1996. Activation of human prefrontal cortex during spatial and object working memory tasks measured by functional MRI. Cereb. Cortex 6, 600–611.

McCarthy, G., Luby, M., Gore, J., Goldman-Rakic, P., 1997. Infrequent events transiently activate human prefrontal and parietal cortex as measured by functional MRI. J. Neurophysiol. 77 (3), 1630–1634.

Medvick, P.A., Lewis, P.S., Aine, C., Flynn, E.R., 1989. Monte-Carlo analysis of localization errors in magnetoencephalography. In: Williamson, S.J., Hoke, M., Stroink, G., Kotani, M. (Eds.), Advances in Biomagnetism. Plenum, New York, pp. 543–546.

Mejis, J.W.H., Bosch, F.G.C., Peters, M.J., Lopes da Silva, F.H., 1987. On the magnetic field distribution generated by a dipolar current source situated in a realistically shaped compartment model of the head. Electroencephalogr. Clin. Neurophysiol. 66, 286–298.

Menon, V., Ford, J.M., Lim, K.O., Glover, G.H., Pfefferbaum, A., 1997. Combined event-related fMRI and EEG evidence for temporal–parietal cortex activation during target detection. NeuroReport 8 (14), 3029–3037.

Mesulam, M.M., 1990. Large-scale neurocognitive networks and distributed processing for attention, language, and memory. Ann. Neurol. 28 (5), 597–613.

Milham, M.P., Banich, M.T., Barad, V., 2003. Competition for priority in processing increases prefrontal cortexes involvement in top-down control: an event-related fMRI study of the Stroop task. Cogn. Brain Res. 17, 212–222.

Mima, T., Nagamine, T., Nakamura, K., Shibasaki, H., 1998. Attention modulates both primary and second somatosensory cortical activities in humans: a magnetoencephalographic study. J. Neurophysiol. 80 (4), 2215–2221.

Nelder, J.A., Meed, R., 1965. A simplex method for function minimization. Comput. J. 7, 308–313.

Neshige, R., Luders, H., 1992. Recording of event-related potentials (P300) from human cortex. J. Clin. Neurophysiol. 9, 294–298.

O'Donnel, B.F., Cohen, R.A., Hokama, H., Cuffin, B.N., Lippa, C., Shenton, M.E., Drachman, D.A., 1993. Electrical source analysis of auditory ERP abnormalities in medial temporal lobe post-encephalitic amnestic syndrome. Electroencephalogr. Clin. Neurophysiol. 87, 394–402.

Okada, Y.C., Papuashvili, N., Xu, C., 1996. What can we learn from MEG studies of the somatosensory system of the swine? Electroencephalogr. Clin. Neurophysiol., Suppl. 47, 35–46.

Pantev, C., Bertrand, O., Eulitz, C., Verkindt, C., Hampson, S., Schuierer, G., Elbert, T., 1995. Specific tonotopic organizations of different areas of the human auditory cortex revealed by simultaneous magnetic and electric recordings. Electroencephalogr. Clin. Neurophysiol. 94 (1), 26–40.

Reite, M., Teale, P., Rojas, D.C., Benkers, T.L., Carlson, J., 2003. Anomalous somatosensory cortical localization in schizophrenia. Am. J. Psychiatry 160 (12), 2148–2153.

Rogers, R.L., Papanicolaou, A.C., Baumann, S.B., Eisenberg, H.M., 1992. Late magnetic fields and positive evoked potentials following infrequent and unpredictable omissions of visual stimuli. Electroencephalogr. Clin. Neurophysiol. 83 (2), 146–152.

Romani, G.L., 1986. Tonotopic organization of the human auditory cortex revealed by steady state neuromagnetic measurements. Acta. Otolaryngol., Suppl. 432, 33–34.

Rosen, I., Asanuma, H., 1972. Peripheral afferent inputs to the forelimb area of the monkey motor cortex: input–output relations. Exp. Brain Res. 14, 257–273.

Sarvas, J., 1987. Basic mathematical and electromagnetic concepts of the bio-magnetic inverse problems. Phys. Med. Biol. 32, 11–22.

Schlitt, H., Heller, L., Aaron, R., Best, E., Ranken, D., 1995. Evaluation of boundary element method for the EEG forward problem: effect of linear interpolation. IEEE. Trans. Biomed. Eng. 42, 52–58.

Sekihara, K., Poeppel, D., Marantz, A., Koizumi, H., Miyashita, Y., 1997. Noise covariance incorporated MEG-MUSIC algorithm: a method for multiple-dipole estimation tolerant of the influence of background brain activity. IEEE Trans. Biomed. Eng. 44 (9), 839–847.

Sekihara, K., Poeppel, D., Marantz, A., Koizumi, H., Miyashita, Y., 1999. MEG spatio-temporal analysis using a covariance matrix calculated from nonaveraged multiple-epoch data. IEEE Trans. Biomed. Eng. 46 (5), 515–521.

Shih, J.J., Weisend, M.P., Davis, J.T., Huang, M., 2000. Magnetoencephalographic characterization of sleep spindles in humans. J. Clin. Neurophysiol. 17 (2), 224–231.

Simoes, C., Jensen, O., Parkkonen, L., Hari, R., 2003. Phase locking between human primary and secondary somatosensory cortices. Proc. Natl. Acad. Sci. U. S. A. 100 (5), 2691–2694.

Simson, R., Vaughan, H.G., Ritter, W., 1976. The scalp topography of potentials associated with missing visual or auditory stimuli. Electroencephalogr. Clin. Neurophysiol. 40, 33–42.

Smith, M.E., Halgren, E., Sokolik, M., Baudena, P., Mussolino, A., Liégeois-Chauvel, C., Chauvel, P., 1990. The intracranial topography of the P3 event-related potential elicited during auditory oddball. Electroencephalogr. Clin. Neurophysiol. 76, 235–248.

Smith, E.E., Jonides, J., Koeppe, R.A., Awh, E., Schumacher, E.H., Minoshima, S., 1995. Spatial versus object working memory: PET investigations. J. Cogn. Neurosci. 7, 337–356.

Snyder, E., Hillyard, S.A., Galambos, R., 1980. Similarities and differences among the P3 waves to detected signals in three modalities. Psychophysiology 17, 112–122.

Spiegel, J., Tintera, J., Gawehn, J., Stoeter, P., Treede, R.D., 1999. Functional MRI of human primary somatosensory and motor cortex during median nerve stimulation. Clin. Neurophysiol. 110 (1), 47–52.

Stapleton, J.M., Halgren, E., 1987. Endogenous potentials evoked in simple cognitive tasks: depth components and task correlates. Electroencephalogr. Clin. Neurophysiol. 67, 44–52.

Stephen, J.M., Aine, C.J., Christner, R.F., Ranken, D., Huang, M., Best, E., 2002. Central versus peripheral visual field stimulation results in timing differences in dorsal stream sources as measured with MEG. Vis. Res. 42 (28), 3059–3074.

Stephen, J.M., Davis, L.E., Aine, C.J., Ranken, D., Herman, M., Hudson,

D., Huang, M., Poole, J., 2003. Investigation of the normal proximal somatomotor system using magnetoencephalography. Clin. Neurophysiol. 114 (10), 1781–1792.

Stevens, A.A., Skudlarski, P., Gatenby, J.C., Gore, J.C., 2000. Event-related fMRI of auditory and visual oddball tasks. Magn. Reson. Imaging 18 (5), 495–502.

Talairach, J., Tournoux, P., 1988. Co-Planar Stereotactic Atlas of the Human Brain. Thieme Medical Publishers Inc, Stuttgart.

Tarkka, I.M., Stokic, D.S., Basile, L.F.H., Papanicolaou, A.C., 1995. Electric source localization of the auditory P300 agrees with magnetic sources localization. Electroencephalogr. Clin. Neurophysiol. 96, 538–845.

Turetsky, B.I., Colbath, E.A., Gur, R.E., 1989a. P300 subcomponent abnormalities in schizophrenia: I. Physiological evidence for gender and subtype specific differences in regional pathology. Biol. Psychiatry 43, 84–96.

Turetsky, B.I., Colbath, E.A., Gur, R.E., 1989b. P300 subcomponent abnormalities in schizophrenia: II. Longitudinal stability and relationship to symptom change. Biol. Psychiatry 43, 331–339.

Urbano, A., Babiloni, F., Babiloni, C., Ambrosini, A., Onorati, P., Rossini, P.M., 1997. Human short latency cortical responses to somatosensory stimulation. A high resolution EEG study. NeuroReport 8 (15), 3239–3243.

Wang, J., Hiramatsu, K.-I., Hokama, H., Miyazato, H., Ogura, C., 2003. Abnormalities of auditory P300 cortical current density in patients with schizophrenia using high density recording. Int. J. Psychophysiol. 47, 243–253.

Wikström, H., Roine, R.O., Salonen, O., Aronen, H.J., Virtanen, J., Ilmoniemi, R.J., Huttunen, J., 1997. Somatosensory evoked magnetic fields to median nerve stimulation: interhemispheric differences in a normal population. Electroencephalogr. Clin. Neurophysiol. 104 (6), 480–487.

Wong, Y.C., Kwan, H.C., MacKay, W.A., Murphy, J.T., 1978. Spatial organization of precentral cortex in awake primates: I. Somato-sensory inputs. J. Neurophysiol. 41, 1107–1120.

Wood, C.C., Cohen, D., Cuffin, B.N., Yarita, M., Allison, T., 1985. Electrical sources in human somatosensory cortex: identification by combined magnetic and potential recording. Science 227, 1051–1053.

Yamaguchi, S., Knight, R.T., 1991. P300 generation by novel somatosensory stimuli. Electroencephalogr Clin. Neurophysiol. 78 (1), 50–55.

Yingling, C.D., Hosobuchi, Y., 1984. A subcortical correlate of P300 in man. Electroencephalogr. Clin. Neurophysiol. 59 (1), 72–76.

Yoshiura, T., Zhong, J., Shibata, D.K., Kwok, W.E., Shrier, D.A., Numaguchi, Y., 1999. Functional MRI study of auditory and visual oddball tasks. NeuroReport 10 (8), 1683–1688.